· Article · Advances in Polar Science
doi:10.12429/j.advps.2025.0016 December 2025 Vol. 36 No. 4: 356-372

Characteristics of net-collected phytoplankton community structure and its relationship with environmental factors in the Southern Ocean: a case study in the Cosmonaut Sea during austral summer of 2020/2021

ZHOU Zhengyi[1,2], ZHAO Jun[3], Alexander L. VERESHCHAKA[4], SUN Xiaohong[1*] & YANG Guang[2,5*]

[1] Shandong University, Weihai, Weihai 264209, China;
[2] Key Laboratory of Marine Ecology and Environmental Sciences, Institute of Oceanology, Chinese Academy of Sciences, Qingdao 266071, China;
[3] Key Laboratory of Marine Ecosystem Dynamics, Second Institute of Oceanography, Ministry of Natural Resources, Hangzhou 310012, China;
[4] Shirshov Institute of Oceanology, Russian Academy of Sciences, Moscow 117997, Russia;
[5] Laboratory for Marine Ecology and Environmental Science, Qingdao Marine Science and Technology Center, Qingdao 266237, China

Received 24 June 2025; accepted 9 October 2025; published online 30 December 2025

Abstract Phytoplankton play a pivotal role in the Southern Ocean ecosystem. This study examines the phytoplankton community structure and the environmental factors driving it in the Cosmonaut Sea, based on samples collected using a net during the summer of 2020/2021. We identified 99 phytoplankton species, predominantly comprising diatoms and dinoflagellates. Among these, diatoms—notably *Pseudo-nitzschia*, *Chaetoceros*, and *Fragilariopsis*, dominated the community in terms of species richness, abundance, and biomass. Endemic species of the Southern Ocean, such as *Corethron pennatum*, *Proboscia alata*, and *Cylindrotheca closterium*, also made significant contributions. Phytoplankton abundance and biomass showed similar spatial distribution patterns, with hotspots in the northern section of the survey area that gradually diminished towards the coastal regions. The oceanic area exhibited low phytoplankton diversity but pronounced regional variations in community distribution, with the northern region emerging as a key zone for abundance, biomass, and diversity. Nutrient distribution was identified as the primary environmental driver shaping the phytoplankton community, with silicate levels having a significant negative impact on overall phytoplankton abundance and the dominant species.

Keywords **Southern Ocean, Cosmonaut Sea, phytoplankton, biomass, community structure, environmental factors**

Citation: Zhou Z Y, Zhao J, Vereshchaka A L, et al. Characteristics of net-collected phytoplankton community structure and its relationship with environmental factors in the Southern Ocean: a case study in the Cosmonaut Sea during austral summer of 2020/2021. Adv Polar Sci, 2025, 36(4): 356-372, doi: 10.12429/j.advps.2025.0016

* Corresponding authors. ORCID:0000-0003-2024-0346. E-mail: sunxiaohong@sdu.edu.cn (SUN Xiaohong). ORCID: 0000-0002-9410-0189. E-mail: yangguang@qdio.ac.cn (YANG Guang)

1 Introduction

Phytoplankton as the key primary producers in marine ecosystems, are essential for maintaining the balance and function of marine ecosystems (Cloern et al., 2014). Through photosynthesis, phytoplankton form the foundation of nearly all marine food webs, significantly impacting the productivity of marine ecosystems. Concurrently, owing to their rapid responses to various environmental disturbances and high biological diversity, phytoplankton serve as excellent ecological indicators for environmental perturbations (Rodrigues et al., 2015). They represent the fundamental basis of the Southern Ocean food web and the primary mechanism for carbon export in this region (Biggs et al., 2021; Deppeler and Davidson, 2017). Thus, understanding changes in phytoplankton community structure and their regulatory factors is crucial for elucidating their responses to climate change and for comprehending the marine ecosystem of the Southern Ocean (Ferreira et al., 2020).

The Southern Ocean generally refers to the region south of the subtropical front (Deppeler and Davidson, 2017). In addition to usual spatiotemporal fluctuations (Orsi et al., 1995), environmental factors show climate-driven changes such as increased ocean temperatures, poleward shift of ocean fronts, and seasonal variability of sea ice, which have profoundly impacted the Antarctic and its marine ecosystem in recent years (Constable et al., 2014, Lee et al., 2022; Mendes et al., 2012). In-depth research on the phytoplankton of the Southern Ocean commenced in the 1930s (Gran, 1931). Early studies identified that the Southern Ocean is characterized by persistent high nutrient concentrations and seasonal high light inputs. This region is recognized as the largest High Nutrient, Low Chlorophyll region (Deppeler and Davidson, 2017; Lee et al., 2012), with its most common ecological system consisting of a short food chain involving diatoms, krill, and higher consumers such as fish, whales and seals (Garibotti et al., 2003). Factors such as iron, light exposure, nutrient-availability, grazing pressure, mixed layer, and viral lysis are considered as regulators of primary productivity in the Southern Ocean (Bazzani et al., 2023; Biggs et al., 2021, 2022; Gutiérrez-Rodríguez et al., 2023). In the extensive Southern Ocean region, phytoplankton have been mostly studied in the broad waters of the West Antarctic, where communities are dominated by large diatoms and *Phaeocystis*. The dynamics of sea ice and meltwater are considered the main factors shaping phytoplankton in this sea area (Ferreira et al., 2020; Lee et al., 2022; Nardelli et al., 2023). The research in the East Antarctic has primarily focused on the Prydz Bay area. Since the establishment of Australia's Davis Station in the Prydz Bay area in 1957, there has been a basic understanding of the distribution of chlorophyll in surface seawater, primary productivity, phytoplankton community structure, and controlling factors in this area (Deppeler et al., 2020; Hancock et al., 2018; Herraiz-Borreguero et al., 2016). The depth of the mixed layer in this sea area, the Antarctic continental slope front, seasonal variations and iron consumption have driven the distribution of phytoplankton dominated by *Fragilariopsis* and *Pseudo-nitzschia* (Heidemann et al., 2024).

The Cosmonaut Sea (30°E to 60°E), situated in the Indian Sector of the Southern Ocean and to the west of Enderby Land in East Antarctic (Hunt et al., 2007), constitutes an integral component of the Southern Ocean's ecological system. Variations in sea ice and surface sea temperatures in this area remain relatively stable (Comiso et al., 2017). The retreat of the West Antarctic Ice Sheet is the primary controlling factor driving environmental transformation (Li et al., 2021). The ecosystem is influenced by the three major currents (Figure 1): the Antarctic Slope Current, the Antarctic Circumpolar Current, and the Weddell Gyre (Mou et al., 2021; Yang et al., 2024). These currents not only shape the Cosmonaut Sea's unique marine environment, but also have a profound impact on its ecosystems, especially on phytoplankton. Currently, there is relatively little phytoplankton research in the Cosmonaut Sea (Davidson et al., 2010; Hunt et al., 2007), which limits our ability to fully understand the ecosystem in this area. A preliminary study of phytoplankton in this area was conducted on the BROKE-West voyage, which recorded a diatom bloom in the offshore area, with centric diatoms dominating the biomass, and identified krill predation as the main determinant of its abundance and composition (Davidson et al., 2010). However, the ecosystem state has likely changed since the time of the voyage. In addition, although other studies involve phytoplankton, they mainly focus on zooplankton feeding (Pakhomov and Perissinotto, 1996) and chlorophyll analysis (Demidov et al., 2007, Li Y H et al., 2024), and in-depth studies on phytoplankton structure and spatiotemporal trends are still insufficient. Therefore, in order to better understand the ecosystem dynamics of the Cosmonaut Sea, it is particularly important to further study the community structure and spatial distribution of phytoplankton.

Both quantitative methods (e.g. bottle sampling) and semi-quantitative methods (e.g. net sampling) are widely used for collecting marine phytoplankton (Davies et al., 2016). Among them, net-based phytoplankton sampling can effectively collect larger phytoplankton samples, which is suitable for large-scale sampling (Jiang et al., 2020). Consequently, based on samples collected from the upper ocean layer (0–200 m) of the Cosmonaut Sea during January 2020, we analyzed the community structure of the net-collected phytoplankton in the Cosmonaut Sea. By describing the species composition, abundance, spatiotemporal distribution, dominant species, community structure, and the role of environmental factors on the phytoplankton in this region, this research aims to further supplement and expand the phytoplankton data in the Cosmonaut Sea, providing foundational data and scientific

basis for subsequent research and development in this area.

2 Materials and methods

2.1 Survey area, sample collection and environmental factors

In January 2021, 37th Chinese Antarctic expedition comprehensively surveyed 25 research stations in the Cosmonaut Sea (33°E–73°E, 62°S–67°S) (Figure 1).

Phytoplankton were collected and analyzed in accordance with the Chinese "Specifications for oceanographic survey—Part 6: marine biological Survey Specifications" (GB/T 12763.6—2007). A small plankton net (with a mesh size of 77 μm, conical shape, and a net opening diameter of 37 cm) was deployed from near the seabed at a depth of 200 m and dragged vertically towards the surface of the sea at a stable speed of 0.5 $m \cdot s^{-1}$. This plankton net was equipped with an electronic flow meter, which was used to calculate the volume of the filtered water. The collected samples were placed in sample bottles and preserved with a buffered 5% formalin solution, and stored in the dark. After thorough mixing, 0.5 mL of the sample was placed in a phytoplankton counting chamber where species were identified and counted under a microscope. The microscope used was the Nikon Eslipse E200 MV, with a magnification of 400 times. The counting chamber type employs a 0.5 mL Utermöhl plankton counting frame. Based on the criterion of identifying at least 500 phytoplankton cells per sample, 1 to 4 replicate experiments were conducted.

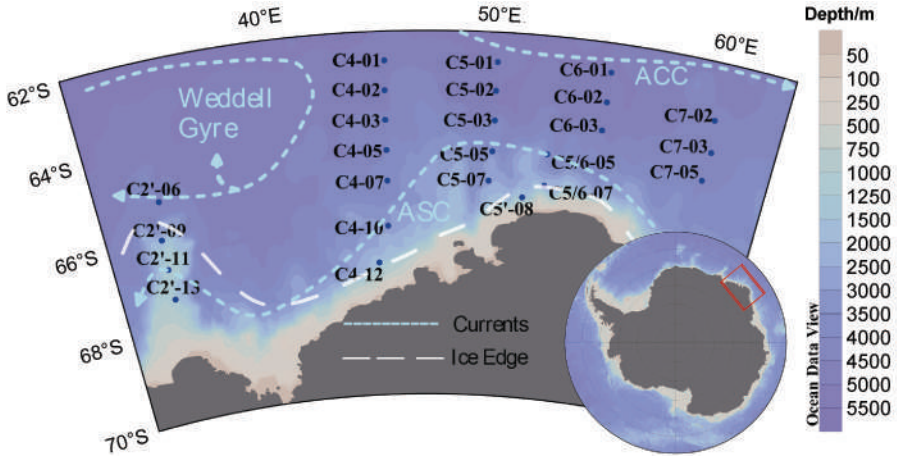

Figure 1 Cosmonaut Sea survey stations during the 2020/2021 austral summer. ACC indicates the Antarctic Circumpolar Current; ASC indicates the Antarctic Slope Current.

Environmental factors are shared data for voyages. Temperature and salinity were measured and recorded using the pre-calibrated Sea-Bird SBE-9/11 plus CTD system (Guo et al., 2023). Water samples were collected with Niskin bottles from different layers (surface, 50 m, 100 m and 200 m) at each station for nutrient analysis. Ammonium concentration was determined using the indophenol blue photometric method, while nitrate, nitrite, phosphate, and silicate concentrations were measured using the cadmium-copper column reduction diazo method, diazo azo method, phosphomolybdenum blue method, and silicon-molybdenum blue method, respectively (Huang et al., 2022). Data for the specific environmental factors can be found in Guo et al. (2023) and Huang et al. (2022). Sea ice data were obtained from the Sea Ice Today (https://nsidc.org/data/NSIDC-0079/versions/3), produced by the U.S. National Snow and Ice Data Center. The spatial resolution of the data was 25 km × 25 km and sea ice extent data for investigation period were selected.

2.2 Data analysis

Abundance was calculated by dividing the number of individuals by the filtration volume, and biomass was estimated by multiplying abundance by the biomass of a single individual. The biomass of a single individual (as carbon content, μg C ind^{-1}) was estimated by: (a) measuring the average cellular volume of ⩾50 individuals per dominant species using geometric approximations; (b) converting biovolume to carbon content using published conversion factors (Menden-Deuer and Lessard, 2000; Yang et al., 2022).

Phytoplankton species diversity was quantified using the Shannon-Wiener diversity index (H', base 2) (MacArthur, 1955):

$$H' = -\sum_{i=1}^{S} P_i \log_2 P_i$$

where S is the total number of species in the sample; $P_i = n_i/N$, n_i is the number of individuals of species i, N is the sum of individuals of all species within the community.

Evenness was assessed using Pielou's Evenness Index (J) (Pielou, 1966):

$$J = H'/\log_2 S$$

where S is the total number of species in the sample.

Species dominance was evaluated using McNaughton's Dominance Index (Y) (McNaughton, 1967):

$$Y = (n_i / N) \times f_i$$

where n_i is the number of individuals of species I; N is the total number of individuals observed; and f_i is the frequency of occurrence of the i-th species across all samples. Species with Y>0.2 are recognized as dominant species that collectively contribute the majority of community biomass and exhibit significant responses to environmental gradients (Xu and Chen, 1989).

Generalized Linear Mixed Models (GLMM) were run to investigate the relationship between different combinations of environmental factors and phytoplankton abundance:

Phytoplankton ~ environmental factor 1 + factor 2 + ⋯ + factorn+ (1 | Site) + (1 | Time)

In the model, (1|Site) and (1|Time) represented the random intercepts for sites and time, respectively. The model employs a negative binomial distribution and is fitted using the glmmTMB package in R (R Core Team, 2024).

The distribution map of phytoplankton abundance is plotted using ODV4 (Schlitzer, 2012). The phytoplankton data were fourth-root transformed using PRIMER v6 (Clarke and Gorley, 2006), followed by the construction of a Bray-Curtis similarity matrix for cluster analysis and non-metric multidimensional scaling. Variance analysis (ANOVA) and Pearson correlation analysis were conducted between phytoplankton cell abundance and environmental factors using IBM SPSS 25 Statistics software (IBM Corp, 2017). The heat map was generated using ChiPlot (https://www.chiplot.online).

GLMM analysis utilized the R programming language. The abundance data of dominant phytoplankton species were examined using Detrended Correspondence Analysis (DCA) with Conoco 5 (ter Braak and Smilauer, 2002). If the gradient length of the first DCA axis was less than 3, redundancy analysis (RDA) was applied to evaluate the relationship between species abundance and environmental factors. Conversely, if the length exceeded 4, Canonical Correlation Analysis (CCA) was employed.

3 Results

3.1 Environmental factors

Among environmental factors, the surface distribution pattern is similar to those of the water column within the 0–200m range, dissolved oxygen and silicate concentrations exhibited a decreasing trend from the southern shore to the north, while temperature, salinity, and other nutrients showed an opposite trend (Figure 2).

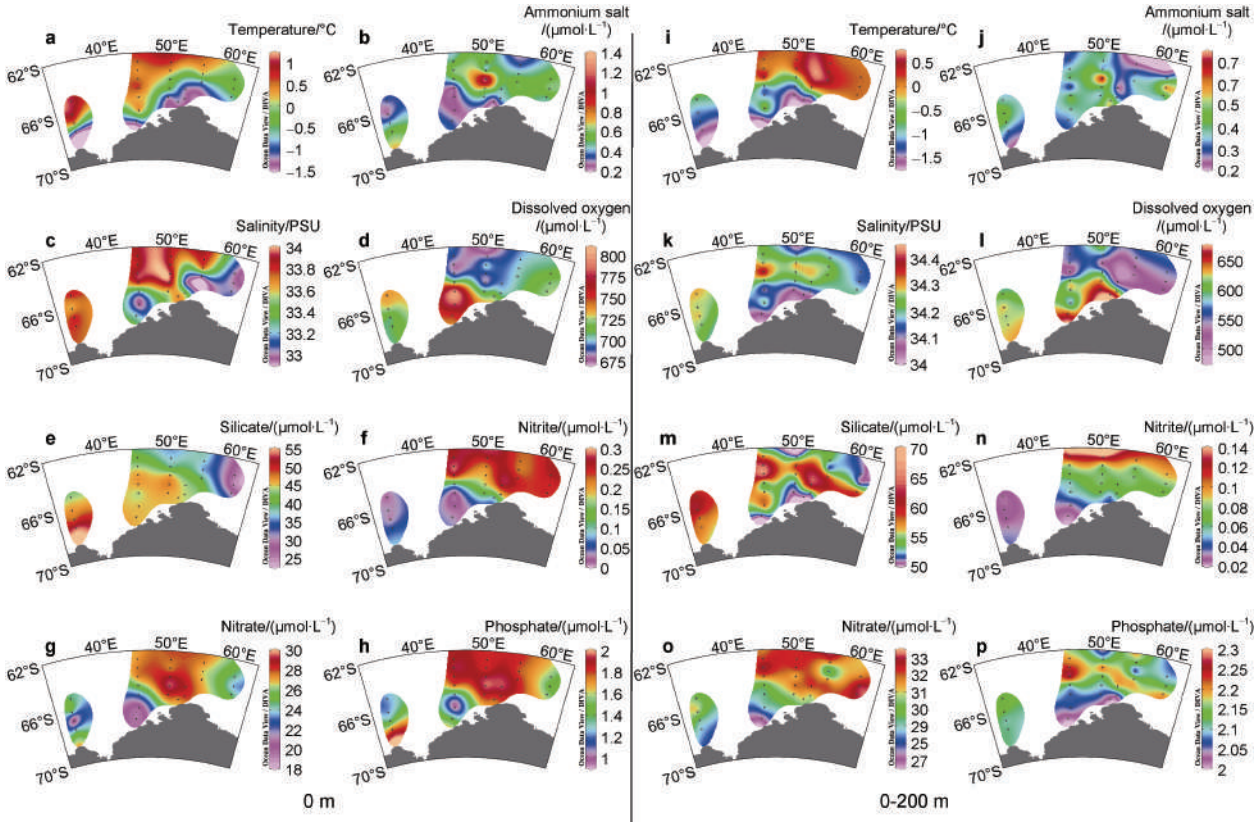

Figure 2 The spatial distribution of environmental factors in the surface layer (**a**–**h**) and 0–200m of water column (**i**–**p**) during the 2020/2021 summer season in the Cosmonaut Sea. **a**, temperature; **b**, ammonium salt concentration; **c**, salinity; **d**, dissolved oxygen; **e**, silicate concentration; **f**, nitrite concentration; **g**, nitrate concentration; **h**, phosphate concentration; **i**–**p**, same as **a**–**h** but for 0–200 m water column. Black bots refer to sampling stations. Off-site data were populated using the DIVA gridding.

3.2 Species composition and dominant species

During the Antarctic expedition in the Cosmonaut Sea, a total of 99 species of phytoplankton from 40 genera across 3 phyla were collected, the diatoms accounted for an absolute majority, with 29 genera and 73 species collected, representing 73.74% of the total phytoplankton species. The Dinophyceae contributed 10 genera and 24 species, constituting 24.24% of the total phytoplankton species, and the Prymnesiophyceae were represented by 1 genus with 2 species. Diatoms were identified as the predominant functional group in the net-collected phytoplankton of the Cosmonaut Sea. The mean abundance and biomass of specific phytoplankton species can be found in Table S1.

All dominant phytoplankton species (Y>0.02) collected during this Antarctic expedition were diatoms (Table 1). *Chaetoceros dichaeta* (Y=0.18) was identified as the most dominant species in the net-collected phytoplankton of the area (Table 1). Other dominant species included *Pseudo-nitzschia lineola*, *Chaetoceros atlanticus*, and *Chaetoceros curvisetus* (Table 1). The genus *Chaetoceros* was found to be the primary contributor to phytoplankton abundance in the Cosmonaut Sea, while *P. alata* was recognized as the main contributor to the biomass (Table 1).

Table 1 Dominant phytoplankton species in net samples

Dominant species	Mean abundance /(cells·L^{-1})	Mean Biomass /($\times 10^4$ μg C·L^{-1})	Degree of dominance (Y)
Chaetoceros dichaeta	1326.01±1358.87	29.63±30.36	0.18
Pseudo-nitzschia lineola	1042.99±997.48	4.85±4.64	0.14
Chaetoceros curvisetus	713.33±957.69	8.69±11.67	0.10
Chaetoceros atlanticus	750.21±1168.58	22.94±35.74	0.10
Fragilariopsis curta	454.84±661.43	2.32±3.37	0.06
Chaetoceros bulbuosus	302.50±386.00	3.28±4.19	0.04
Pseudo-nitzschia prolongatoides	290.60±325.56	282.66±316.66	0.04
Fragilariopsis kerguelensis	317.33±591.80	4.79±8.93	0.04
Proboscia alata	316.61±471.20	0.62±0.93	0.04
Corethron pennatum	201.80±169.80	34.8±29.28	0.03
Cylindrotheca closterium	198.04±273.40	0.30±0.42	0.03
Chaetoceros concavicornis	181.32±162.79	8.92±8.00	0.03

3.3 Species composition and distribution patterns of abundance and biomass

The phytoplankton cell abundance ranged from 5.76 to 1.71×10^4 cells·L^{-1}, with an average abundance of $(7.21\pm 5.71)\times10^3$ cells·L^{-1}. The biomass ranged from 0.08×10^6 to 20.44×10^6 μg C·L^{-1}, with an average biomass of $(6.60\pm5.92)\times10^6$ μg C·L^{-1}. The high abundance areas of net-collected phytoplankton were primarily located in the northeastern part of the surveyed region, with the highest values observed at station C7-02 (Figure 3a). The high biomass areas were distributed in the northern part of the survey area, decreasing southward towards the coast (Figure 3b). The western part of the region had overall lower abundance and biomass (Figures 3a and 3b), with diatoms showing similar distribution trends to the overall phytoplankton community (Figures 3a–3d). The western area of the survey region was a high-value zone for both abundance and biomass of dinoflagellates, which also showed a decreasing trend towards the coast, while the central sea area had lower abundance and biomass of dinoflagellates with a more scattered distribution (Figures 3e and 3f).

The dominant phytoplankton species were *C. dichaeta* (Y=0.18) and *P. lineola* (Y=0.14), with average abundances of 1,326.01 cells·L^{-1} and 1,042.99 cells·L^{-1}, respectively. These species accounted for 18% and 14% of the total phytoplankton abundance, with biomass values of 296300.17 μg C·L^{-1} and 48510.64 μg C·L^{-1}, respectively. The distribution of the two species was similar, with high-value areas being quite patchy and a general trend of decreasing from the northeast to the southwest (Figures 4a and 4b). Additionally, *C. curvisetus* (Y=0.10) and *C. atlanticus* (Y=0.10) were also major dominant species in the area. The high-value areas for *C. curvisetus* were located in the mid-coastal and northeastern parts of the surveyed sea area, with lower abundance in the western sea areas (Figure 4c). In contrast, the high-value areas for *C. atlanticus* were found in the northeastern part of the surveyed sea area, showing a decreasing trend towards the western coast (Figure 3d).

3.4 Species diversity

The Shannon-Wiener diversity index (H') for phytoplankton ranged from 0.98±0.10, while Pielou's evenness index (J) ranged from 0.61±0.08. The diversity of phytoplankton was low and the distribution of all species was uniform. The horizontal distribution shows that the Shannon-Wiener diversity index was generally low, with a trend of decreasing towards the shore in the southwestern part of the surveyed area (Figure 5a). The high-value area of Pielou's evenness index was observed in the northern part of the surveyed sea area, the index decreased towards the shore, especially in the southwest coastal waters (Figure 5b).

3.5 Community structure

At a similarity level of approximately 67%, the phytoplankton community in the Cosmonaut Sea during the 2020/2021 summer season could be delineated into 5 distinct clusters (Figure 6a). Cluster a was located in the southern part of the surveyed area, with *F. curta* as the dominant species; Cluster b was situated in the southwestern part of the surveyed area, where *Alexandrium* sp., *Dinophysis acuminata*, and *F. curta* were the primary dominant species; Cluster c was found in the southern

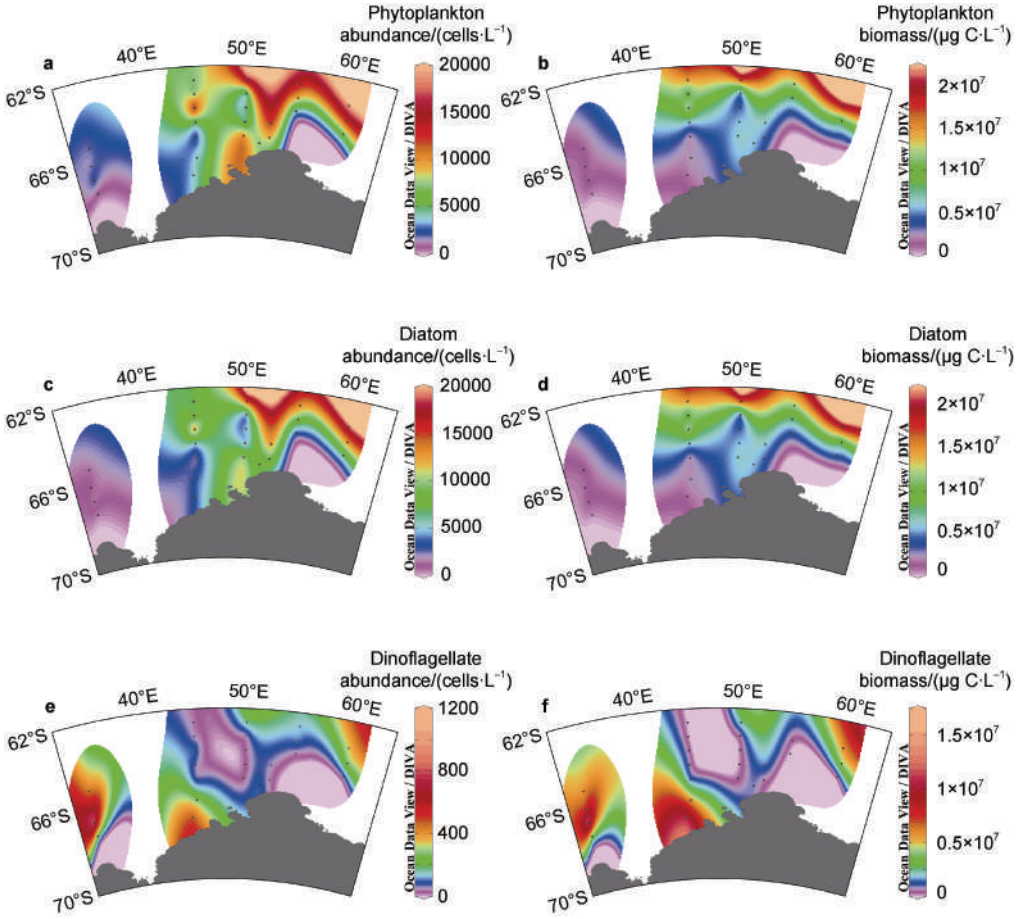

Figure 3 The spatial distribution of the net-collected phytoplankton abundance (cells·L^{-1}) and biomass (μg C·L^{-1}) in the top 200 m of the Cosmonaut Sea during the 2020/2021 summer season. **a**, phytoplankton abundance; **b**, phytoplankton biomass; **c**, diatom abundance; **d**, diatom biomass; **e**, dinoflagellate abundance; **f**, dinoflagellate biomass. Black dots refer to sampling stations. Off-site data were generated using the DIVA gridding.

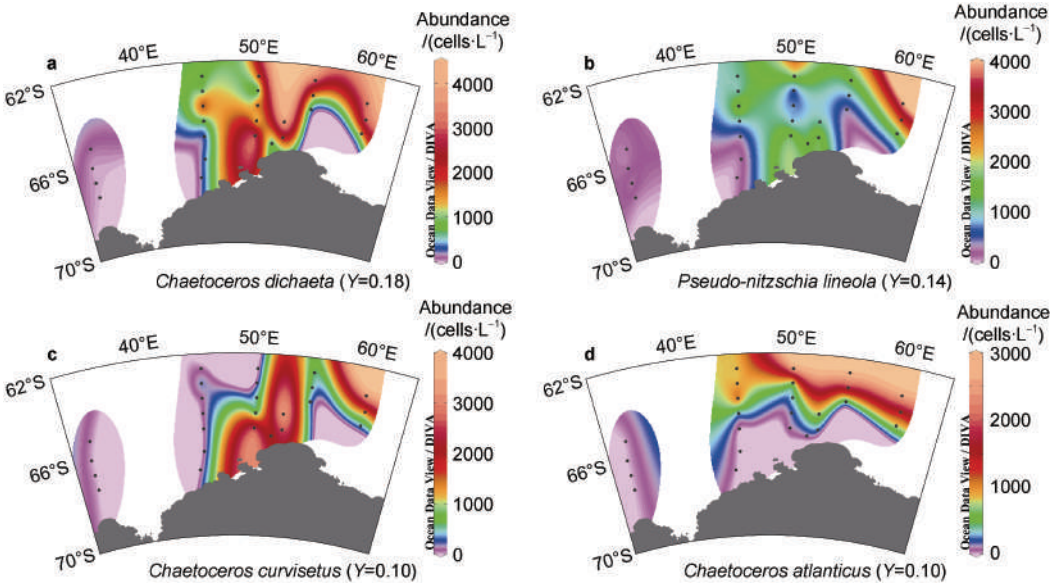

Figure 4 The spatial distribution of dominant the net-collected phytoplankton species in the 0–200m water column of the Cosmonaut Sea. **a**, *Chaetoceros dichaeta* (*Y*=0.18); **b**, *Pseudo-nitzschia lineola* (*Y*=0.14); **c**, *Chaetoceros curvisetus* (*Y*=0.10); **d**, *Chaetoceros atlanticus* (*Y*=0.10). Black bots refer to sampling stations. Off-site data were generated using the DIVA gridding.

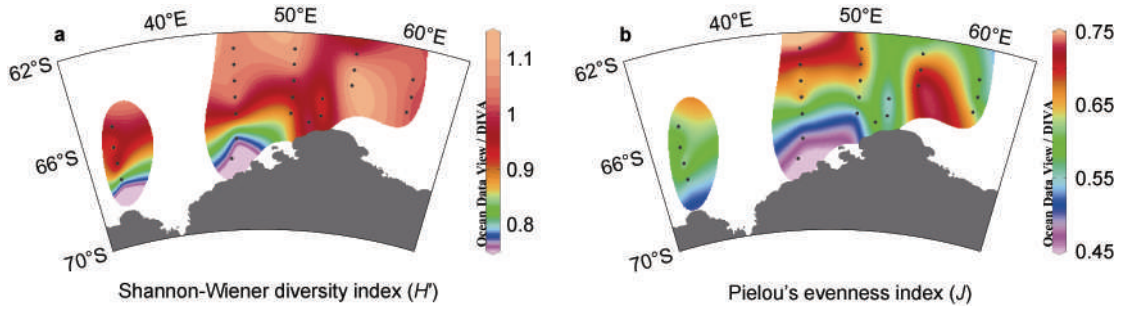

Figure 5 The spatial distribution of the net-collected phytoplankton diversity indices in the 0–200 m water column of the Cosmonaut Sea. **a**, Shannon-Wiener diversity index; **b**, Pielou's evenness index. Black bots refer to sampling stations. Off-site data were populated using the DIVA gridding.

coastal areas of the surveyed region, with *C. curvisetus* and *C. dichaeta* being the main dominant species; Cluster d was near station C5-05, where *P. lineola*, *P. alata*, and *C. dichaeta* were the predominant species; Cluster e was in the northern part of the surveyed area, with *C. dichaeta*, *P. lineola*, and *C. atlanticus* being the key dominant species (Figure 6b).

Based on the proximity to the shore, distinct communities have formed in this maritime region, with the northern survey areas constituting a uniform group located in the high-value zones for abundance, biomass, diversity, and other distributional aspects (Figure 6b). In contrast, the nearshore areas exhibit a gradient of diverse communities from west to east (Figure 6b).

3.6 Effects of environmental factors on phytoplankton

3.6.1 Correlation analysis between phytoplankton and environmental factors

The abundance of phytoplankton and diatoms in the Cosmonaut Sea showed a significant negative correlation with surface silicate concentrations, a significant positive correlation with surface and 0–200 m water column nitrites, and a significant positive correlation with 0–200 m water column temperature (Figure 7). Dinoflagellate showed significant negative correlation with surface nitrate and phosphate, significant negative correlation with surface nitrite, and significant negative correlation with 0–200 m seawater water column (Figure 7).

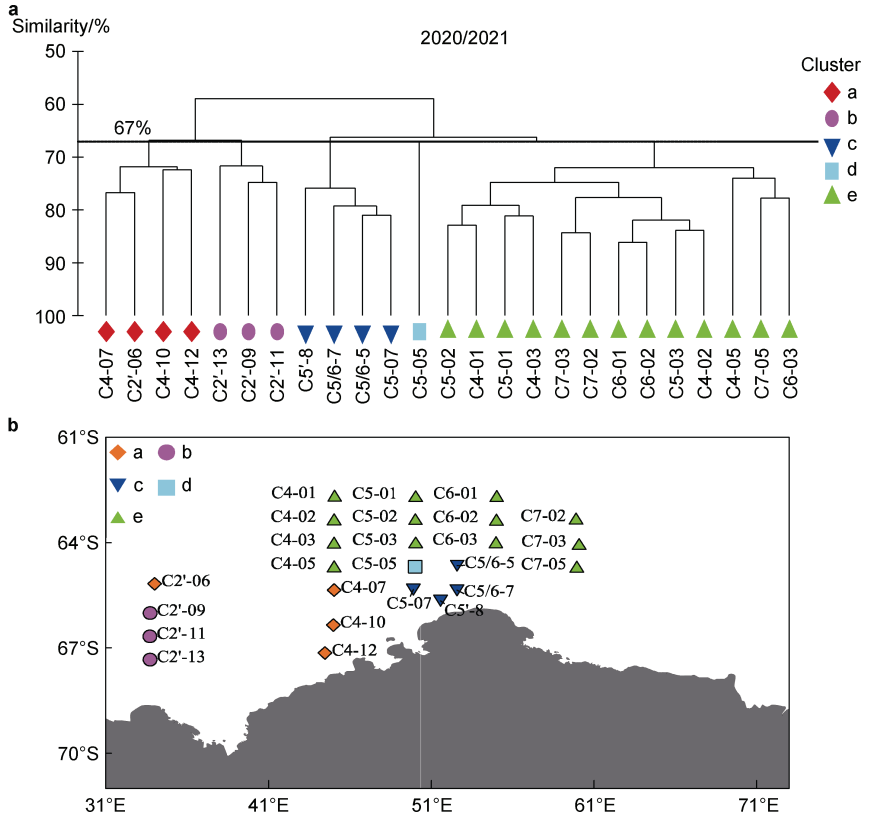

Figure 6 The net-collected phytoplankton community clustering analysis (**a**) and spatial distribution (**b**) in the Cosmonaut Sea.

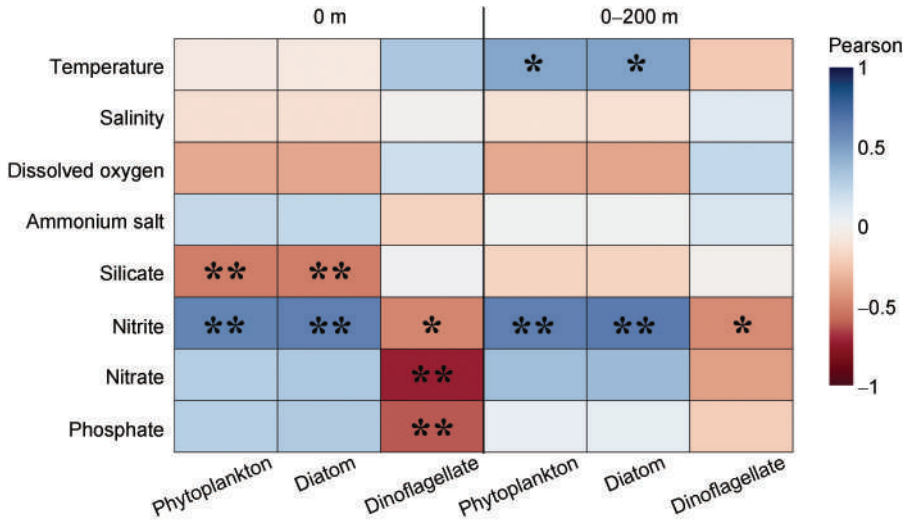

Figure 7 The correlation analysis between the net-collected phytoplankton and environmental factors in the Cosmonaut Sea. Notes: **, at the 0.01 level (two-tailed), the correlation is highly significant; *, at the 0.05 level (two-tailed), the correlation is significant.

GLMMs were run with phytoplankton abundance as the response variable, environmental factors as fixed effects, and sampling sites and times as random effects. Pearson correlation analysis revealed that phytoplankton abundance was significantly correlated with nitrite and silicate at the 0 m layer (p<0.01) (Figure 7). Subsequent model fitting indicated overdispersion (overdispersion> 1.5), suggesting that a negative binomial distribution was more appropriate. Similarly, in the 0–200 m water column, phytoplankton abundance was significantly correlated with nitrite (p<0.01), while a significant correlation was observed with temperature (p<0.05) (Figure 7). The corresponding model further exhibited overdispersion (overdispersion>1.5), reinforcing the suitability of a negative binomial distribution.

In the analysis of the surface layer models, GLMMs with fixed effects of nitrite alone, nitrite and silicate together, and the interaction between nitrite and silicate showed good fit (Table S2). The differences in Akaike Information Criterion among these three models were less than 2, indicating no significant differences in model fit (Table S2). This suggests that nitrite has a significant impact on phytoplankton abundance, and the combined effect of nitrite and silicate also significantly influenced phytoplankton abundance, suggesting a potential interaction between these two factors. In contrast, the model with silicate alone exhibited poor fit (Table S2), implying that the effect of silicate may depend on the presence of nitrite. Based on the principle of parsimony, the model with nitrite alone was selected as the best model. Analysis of its effect plot revealed that a positive coefficient for the fixed factor corresponded to an increasing fitted curve, indicating a positive influence on phytoplankton abundance (Figure S1). The increasing slope of the curve and the widening confidence interval suggest that as the relative concentration of nitrite increases, its impact on phytoplankton abundance becomes stronger, although the estimation precision decreases (Figure S1). In the analysis of the 0–200 m water column models, the GLMM with fixed effects of nitrite alone exhibited a good fit. The fitted curve increased as the factor value increased, indicating a significant positive effect of nitrite on phytoplankton abundance (Table S2 and Figure S1).

3.6.2 Redundancy analysis of dominant species and environmental factors

A DCA was conducted, and since the gradient of the first axis was less than 3, an RDA was performed between the abundance of each dominant species and environmental factors. The first ordination axis in each summer showed significant differences from the remaining axes (p<0.05), indicating the reliability of the RDA results.

The analysis revealed that, for surface environmental factors, most dominant species showed a negative correlation with silicate, while being positively correlated with multiple of nutrients (Figure 8). The most dominant species of phytoplankton, *C. dichaeta*, collected by net sampling in this sea area, showed a significant positive correlation with nitrate (Figure 8). *F. curta* was positively correlated with dissolved oxygen, and *C. curvisetus* showed a negative correlation with temperature and salinity (Figure 8). For the 0–200 m water column environmental factors, most dominant species were positively correlated with temperature, nitrite, and nitrate (Figure 8).

It was evident that the cell abundance of the summer phytoplankton dominant species in the Cosmonaut Sea was influenced to varying degrees by multiple environmental factors, and their distribution was closely related to various nutrients. The majority of phytoplankton dominant species exhibited similarities in their response to environmental

factors. Through the analysis of the relationship between the cell abundance of phytoplankton dominant species and both surface water and 0–200 m water column environmental factors, differences were observed, which may be related to the spatial distribution differences of the dominant species (Figure 8).

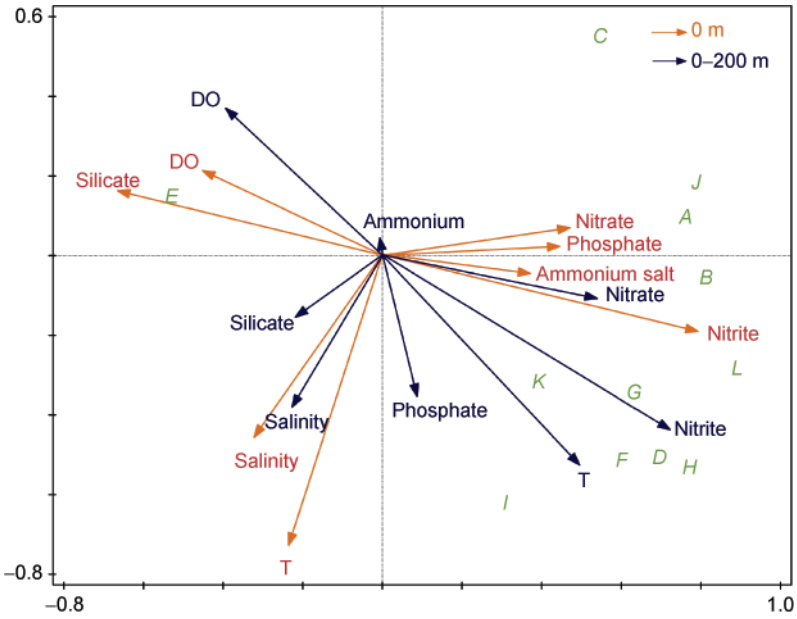

Figure 8 RDA analysis of dominant phytoplankton species and environmental factors in 0 m layer and 0–200 water column. A, *Chaetoceros dichaeta*; B, *Pseudo-nitzschia lineola*; C, *Chaetoceros curvisetus*; D, *Chaetoceros atlanticus*; E, *Fragilariopsis curta*; F, *Chaetoceros bulbuosus*; G, *Pseudo-nitzschia prolongatoides*; H, *Fragilariopsis kerguelensis*; I, *Proboscia alata*; J, *Corethron pennatum*; K, *Cylindrotheca Closterium*; L, *Chaetoceros concavicornis*.

4 Discussion

4.1 Characteristics of phytoplankton community structure

Diatoms constituted the primary functional group in the net-collected phytoplankton of the Cosmonaut Sea, which is consistent with the findings of large diatoms during the BROKE-West voyage (Davidson et al., 2010). The species observed in this survey were primarily long-chained, large-celled diatom species, specifically from the genera *Chaetoceros*, *Pseudo-nitzschia*, and *Fragilariopsis*. Davidson et al. also identified large diatoms, dominated by *Fragilariopsis* spp. and *Chaetoceros* spp., in the water (Davidson et al., 2010). Historical data indicate that diatoms possess a significant advantage within the phytoplankton community of the Southern Ocean (Shramik et al., 2013; Wolf et al., 2013), especially in the Weddell Sea and Prydz Bay adjacent to the survey area. Moreover, diatoms are major contributors to the biomass of large phytoplankton during comparable survey periods (Browning et al., 2021; Deshmukh et al., 2024).

The mesh size of plankton nets significantly influences sample composition (Hernroth, 1987). Net sampling often omits small phytoplankton while overestimating larger or colonial diatoms, potentially biasing abundance reports (Jiang et al., 2020). Consequently, this methodology better captures long-chain, large-celled phytoplankton than water collection methods (Jiang et al., 2020). However, small taxa prevalent in BROKE-West voyage water samples, such as the diatom *Nitzschia*, certain *Gymnodinium* dinoflagellates, and the abundant *Phaeocystis*, may have been underrepresented (Davidson et al., 2010). Such omissions could impact analyses of large phytoplankton via interspecific competition. Net sampling is also susceptible to blockage (Skjoldal et al., 2013), particularly by diatom and *Phaeocystis* cysts (Davidson et al., 2010), which can allow smaller organisms to enter samples in bloom conditions. Furthermore, net sampling may inadequately capture the spatial heterogeneity of phytoplankton communities influenced by water-mass biogeochemistry (e.g. advection and mixing, Zoccarato et al., 2016). This limitation is reflected in our observed differences between phytoplankton abundance relationships with surface versus water-column environmental factors (Figure 7).

In comparison to the global phytoplankton biodiversity reported by Irigoien et al. (2004), the Shannon-Wiener diversity index of phytoplankton in the Cosmonaut Sea was low, indicating the diversity of net-collected phytoplankton is at a low level, which aligns with findings regarding the low native biodiversity in this region (Davidson et al., 2010). Davidson et al. (2010) also observed that the abundance and diversity of large diatoms and dinoflagellates increased only in the coastal waters of this region. However, in the current survey, the diversity index

and evenness index of large phytoplankton in the coastal waters were significantly lower than the average levels.

The phytoplankton exhibited significant regional differences in this survey. Some studies have shown that the spatial distribution of phytoplankton analyzed by net samples is basically consistent with that of water samples (Jiang et al., 2020). Given this, our findings, based on net sampling methods, exhibit both similarities and discrepancies when compared to the results of the BROKE-West voyage, which utilized water sampling methods (Davidson et al., 2010). In this study, two species of dinoflagellate *Alexandrium* sp. and *D. acuminata* were found to dominate the Cluster b in the western part of the survey area. Davidson's analysis also showed that this area lacked long-chained, large-celled phytoplankton species such as *Chaetoceros*, *Thalassiosira*, and *Pseudo-nitzschia*, primarily due to the abundant presence of *Phaeocystis* and unidentified nanoheterotrophic protists (Davidson et al., 2010). In contrast to the findings of Davidson et al. (2010), this survey found that in communities in the central of the survey area, the dominance of *C. dichaeta* and *C. curvisetus* was greater than that of *C. atlanticus*, which was a main dominant species in their study. Moreover, another long-chained dominant species, *Thalassiosira* (Davidson et al., 2010), did not establish dominance in this survey.

4.2 Effects of environmental factors on phytoplankton community structure

Similar to previous studies (Abram et al., 2013), the survey period in our research area coincided with the ice-melting season, which was characterized by an obvious retreat of sea ice. In regions with high sea ice concentration, glacial meltwater input altered surface salinity, promoting the formation of shallow mixed layers and resulting in a northward increase in salinity from the coast (Pan et al., 2020). In ice-free areas, solar radiation continued to serve as a heat source (Allison et al., 1993), in conjunction with the presence of the mixed layer. Additionally, the influence of the Antarctic Slope Current, Weddell Gyre and Antarctic Circumpolar Current facilitated the influx of nutrients, dissolved oxygen, and substantial organic matter, thereby promoting the growth and reproduction of phytoplankton (Moreau et al., 2023).

Generally, the phytoplankton structure is influenced by various factors, including temperature and nutrient availability within the survey area. Temperature can limit the growth of diatoms in the Southern Ocean (Jabre et al., 2021). Westwood et al. (2010) found that lower temperatures associated with meltwater had no adverse effects on primary production. Major nutrients can be limiting factors for phytoplankton growth (Krishnamurthy et al., 2010), with various phytoplankton species exhibiting distinct preferences for specific nutrients. Silicon, a key component of the silicified cell walls of diatoms, is essential for their growth and reproduction (Allen et al., 2005; Martin-Jézéquel et al., 2000). A highly significant negative correlation exists in the survey area between the abundance of phytoplankton and diatoms and surface silicate concentrations likely due to the significant consumption of silicate by diatoms (Figure 8). The survey conducted on the BROKE-West voyage also found that the areas with thriving diatom populations were characterized by low silicate concentrations (Westwood et al., 2010). Nitrogen and phosphorus are also limiting factors for phytoplankton growth and development (Bristow et al., 2017). The optimal N/P ratio for diatoms is 16:1 (Redfield, 1958). Under conditions of low phosphate concentration, diatom growth is more likely to be inhibited compared to other phytoplankton groups. In environments with a high N/P ratio, the competitive ability of diatoms declines (Bi et al., 2021). Most stations in this region had an N/P ratio less than or close to 16:1, therefore increases in inorganic nitrogen and phosphorus can promote phytoplankton growth (Tyrrell, 1999). The differential effects of nitrite and nitrate on phytoplankton in this region, may be related to diatom's selective preference for different forms of nitrogen (Admiraal et al., 1987, Li Z Z et al., 2024). Another possibility is that phytoplankton consume high concentrations of nitrate while releasing nitrite (Collos, 1998), resulting in a highly significant positive correlation between nitrite and phytoplankton abundance. Therefore, nitrate is likely to be a controlling factor for the phytoplankton in this area, whereas low concentrations of nitrite are more suitable for predicting the distribution of phytoplankton.

Additionally, there are similarities in the influence of environmental factors in this study (Table 1 and Figure 8). Notably, the potentially toxic species *Pseudo-nitzschia* sp., which has recently been confirmed to produce the the neurotoxins domoic acid and iso-domoic acid C (Brito-Echeverría et al., 2025; Olesen et al., 2021), shows a positive response to various nutrients (Figure 7). Brito-Echeverría et al. (2025) further demonstrated that eutrophication in Antarctic coastal areas significantly influenced the frequency of harmful algal blooms. Their research also suggested that carbon dioxide, a key environmental factor, can affect domoic acid production by *Pseudo-nitzschia* sp. (Brito-Echeverría et al., 2025). Unlike other dominant species, *F. curta* was significantly influenced by dissolved oxygen levels in seawater and was negatively affected by various nutrients (Figure 8). This phenomenon may stem from the mesh of the sampling net, which can become clogged with long, large phytoplankton diatoms, leading to the extensive capture of smaller, dominant *F. curta*. With their small cell volume and relatively high surface area-to-volume ratio, these small phytoplankton significantly contribute to CO_2 fixation in the Southern Ocean (Irion et al., 2021), and their release of O_2 also varies with abundance. Moreover, the high abundance of *F. curta* often coincides with significant nutrient depletion in the water column (Davidson et al.,

2010), thereby reinforcing the negative correlation of nutrients on net-collected samples.

Distinct communities formed near the coast of the survey area, potentially related to the significant gradient of mixed layer depth from west to east (Westwood et al., 2010). Cluster a locates in this area with the lowest phytoplankton species diversity. The influence of sea ice meltwater (Qi et al., 2025) can elevate dissolved oxygen in this region, stimulating the growth of *F. curta*, while a large number of small algae, such as *Phaeocystis* sp., exist in the water column (Davidson et al., 2010), resulting in low nutrient levels. Cluster b (the western part of the survey area) is associated with a region influenced by the Weddell Gyre and the Antarctic Slope Current where dinoflagellates are the primary dominant species. In particular, toxic phytoplankton like *Alexandrium* sp. and *Dinophysis* sp. exhibit high tolerance to temperature changes, and silicate concentration is likely a key influencing factor (Brito-Echeverría et al., 2025, Ho et al., 2003, Krock et al., 2020). This area is also limited in the growth of diatoms due to the low nitrogen utilization rate (Kolody et al., 2022), resulting in a high concentration of silicate in this region. Cluster e, located further from the coast and sea ice, aligns with historical data (Davidson et al., 2010) and serves as a hotspot for the abundance and biomass of macrocellular, long-chain phytoplankton. Additionally, this area exhibited a high zooplankton abundance during the study period, with the elevated phytoplankton concentrations promoting the reproduction and growth of zooplankton, especially copepods (Mou et al., 2021), which dominated the plankton ecosystem through the top-down effect.

5 Conclusion

Research on the structure of the net-collected phytoplankton and its relationship with environmental factors during the summer of 2020/2021 revealed that the phytoplankton species in Cosmonaut Sea are predominantly composed of diatoms and dinoflagellates, with diatoms being the primary contributors to abundance and biomass. The dominant species in this region are all diatoms, with *C. dichaeta* (Y=0.18) identified as the most prevalent. Other notable genera include *Pseudo-nitzschia*, *Chaetoceros*, and *Fragilariopsis*, characterized by their long chains and large-cell structures. Their larger surface area-to-volume ratio facilitates the absorption of essential nutrients, including nitrogen (N) and phosphorus (P). The abundance and biomass of phytoplankton in this area exhibit a decreasing trend from the northern sea region to the nearshore. Most areas display low species diversity, with particularly low diversity levels noted in the southwest. Furthermore, species distribution is uneven, and the community structure appears fragile. Cluster analysis identified distinct planktonic communities formed in nearshore versus offshore areas. Nearshore communities varied from west to east, while offshore communities were more homogeneous and associated with regions of higher biomass and biodiversity. This pattern is potentially influenced by sea ice meltwater and ocean circulation. The cellular abundance of phytoplankton in this area is closely related to the distribution of various nutrients, particularly silicate and nitrite, with silicate exerting a significant negative impact on both phytoplankton abundance and the composition of dominant species. Our correlation analyses reveal species-specific environmental thresholds governing community assembly—notably *C. dichaeta*'s nitrate dependence and *F. curta*'s sensitivity to dissolved oxygen. These quantifiable relationships significantly improve predictive models of phytoplankton regime shifts under projected climate scenarios, highlighting the need for sustained monitoring of nonlinear interactions between warming-induced stratification and micronutrient limitation.

Acknowledgements We would like to thank the crew on R/V *Xuelong* for their assistance with the plankton sampling. This work was funded by National Science Foundation of China (Grant no. 42276238), Impact and Response of Antarctic Seas to Climate Change (Grant nos. IRASCC 01-02-01D, 01-01-02A) and Taishan Scholars Program. We thank the 3 anonymous reviewers and Guest Editor Dr. Mukan Ji for their helpful comments. The authors report no conflict of interest. The data that support the findings of this study are available from the corresponding author upon reasonable request.

References

Abram N J, Wolff E W, Curran M A J. 2013. A review of sea ice proxy information from polar ice cores. Quat Sci Rev, 79: 168-183, doi:10.1016/j.quascirev.2013.01.011.

Admiraal W, Riaux-Gobin C, Laane R W P M. 1987. Interactions of ammonium, nitrate, and D- and L-amino acids in the nitrogen assimilation of two species of estuarine benthic diatoms. Mar Ecol Prog Ser, 40(3): 267-273, doi:10.3354/meps040267

Allen J T, Brown L, Sanders R, et al. 2005. Diatom carbon export enhanced by silicate upwelling in the northeast Atlantic. Nature, 437(7059): 728-732, doi:10.1038/nature03948.

Allison I, Brandt R E, Warren S G. 1993. East Antarctic sea ice: Albedo, thickness distribution, and snow cover. J Geophys Res Oceans, 98(C7): 12417-12429, doi:10.1029/93JC00648.

Bazzani E, Lauritano C, Saggiomo M. 2023. Southern ocean iron limitation of primary production between past knowledge and future projections. J Mar Sci Eng, 11(2): 272, doi:10.3390/jmse11020272.

Bi R, Cao Z, Ismar-Rebitz S M H, et al. 2021. Responses of marine diatom-dinoflagellate competition to multiple environmental drivers: abundance, elemental, and biochemical aspects. Front Microbiol, 12: 731786, doi:10.3389/fmicb.2021.731786.

Biggs T E G, Huisman J, Brussaard C P D. 2021. Viral lysis modifies seasonal phytoplankton dynamics and carbon flow in the Southern Ocean. ISME J, 15(12): 3615-3622, doi:10.1038/s41396-021-01033-6.

Biggs T E G, Rozema P D, Evans C, et al. 2022. Control of Antarctic phytoplankton community composition and standing stock by light availability. Polar Biol, 45(11): 1635-1653, doi:10.1007/s00300-022-

03094-5.

Bristow L A, Mohr W, Ahmerkamp S, et al. 2017. Nutrients that limit growth in the ocean. Curr Biol, 27(11): R474-R478, doi:10.1016/j.cub.2017.03.030.

Brito-Echeverría J, Pérez P, Echeveste P. 2025. Assessing environmental drivers of toxin-producing cyanobacteria and phytoplankton in Antarctic and sub-Antarctic waters. Polar Biol, 48(2): 57, doi:10.1007/s00300-025-03375-9.

Browning T J, Achterberg E P, Engel A, et al. 2021. Manganese co-limitation of phytoplankton growth and major nutrient drawdown in the Southern Ocean. Nat Commun, 12(1): 884, doi:10.1038/s41467-021-21122-6.

Clarke K R, Gorley R N. 2006. PRIMER v6: User manual/tutorial. Plymouth: PRIMER-E Ltd.https://scirp.org/reference/referencespapers?referenceid=1371182.

Cloern J E, Foster S Q, Kleckner A E. 2014. Phytoplankton primary production in the world's estuarine-coastal ecosystems. Biogeosciences, 11(9): 2477-2501, doi:10.5194/bg-11-2477-2014.

Collos Y. 1998. Nitrate uptake, nitrite release and uptake, and new production estimates. Mar Ecol Prog Ser, 171: 293-301, doi:10.3354/meps171293.

Comiso J C, Gersten R A, Stock L V, et al. 2017. Positive trend in the Antarctic sea ice cover and associated changes in surface temperature. J Clim, 30(6): 2251-2267, doi:10.1175/jcli-d-16-0408.1.

Constable A J, Melbourne-Thomas J, Corney S P, et al. 2014. Climate change and Southern Ocean ecosystems I: how changes in physical habitats directly affect marine biota. Glob Chang Biol, 20(10): 3004-3025, doi:10.1111/gcb.12623.

Davidson A T, Scott F J, Nash G V, et al. 2010. Physical and biological control of protistan community composition, distribution and abundance in the seasonal ice zone of the Southern Ocean between 30 and 80°E. Deep Sea Res Part II Top Stud Oceanogr, 57(9/10): 828-848, doi:10.1016/j.dsr2.2009.02.011.

Davies C H, Coughlan A, Hallegraeff G, et al. 2016. A database of marine phytoplankton abundance, biomass and species composition in Australian waters. Sci Data, 3: 160043, doi:10.1038/sdata.2016.43.

Demidov A B, Vedernikov V I, Sheberstov S V. 2007. Spatiotemporal variability of chlorophyll a in the Altantic and Indian sectors of the Southern Ocean during February–April of 2000 according to satellite and expeditionary data. Oceanology, 47(4): 507-518, doi:10.1134/s000143700704008x.

Deppeler S L, Davidson A T. 2017. Southern ocean phytoplankton in a changing climate. Front Mar Sci, 4: 40, doi:10.3389/fmars.2017.00040.

Deppeler S, Schulz K G, Hancock A, et al. 2020. Ocean acidification reduces growth and grazing impact of Antarctic heterotrophic nanoflagellates. Biogeosciences, 17(16): 4153-4171, doi:10.5194/bg-17-4153-2020.

Deshmukh P D, George J V, Naik R K, et al. 2024. Phytoplankton community structure during the melting phase of the land-fast ice in Prydz Bay, east Antarctica. Polar Sci, 40: 101046, doi:10.1016/j.polar.2024.101046.

Ferreira A, Costa R R, Dotto T S, et al. 2020. Changes in phytoplankton communities along the northern Antarctic Peninsula: causes, impacts and research priorities. Front Mar Sci, 7: 576254, doi:10.3389/fmars.2020.576254.

Garibotti I A, Vernet M, Ferrario M E, et al. 2003. Phytoplankton spatial distribution patterns along the western Antarctic Peninsula (Southern Ocean). Mar Ecol Prog Ser, 261: 21-39, doi:10.3354/meps261021.

Gran H H. 1931. On the conditions for the production of plankton in the sea. Rapports et Procès-Verbaux des réunions, 75(75): 37-46.

Guo J Y, Yang X F, Zhao J, et al. 2023. Distributions of dissolved oxygen and apparent oxygen utilization in the Cosmonaut Sea and Amundsen Sea in austral summer 2021. Adv Polar Sci, 34(4): 272-303, doi:10.12429/j.advps.2023.0007.

Gutiérrez-Rodríguez A, Latasa M, Safi K, et al. 2023. Decoupled growth and grazing rates of diatoms and green algae drive increased phytoplankton productivity on HNLC sub-Antarctic plateaux. Limnol Oceanogr Lett, 8(6): 896-905, doi:10.1002/lol2.10355.

Hancock A M, Davidson A T, McKinlay J, et al. 2018. Ocean acidification changes the structure of an Antarctic coastal protistan community. Biogeosciences, 15(8): 2393-2410, doi:10.5194/bg-15-2393-2018.

Heidemann A C, Westwood K J, Foppert A, et al. 2024. Drivers of phytoplankton distribution, abundance and community composition off East Antarctica, from 55-80°E (CCAMLR Division 58.4.2 East). Front Mar Sci, 11: 1454421, doi:10.3389/fmars.2024.1454421.

Hernroth L. 1987. Sampling and filtration efficiency of two commonly used plankton nets. A comparative study of the Nansen net and the Unesco WP 2 net. J Plankton Res, 9(4): 719-728, doi:10.1093/plankt/9.4.719.

Herraiz-Borreguero L, Lannuzel D, van der Merwe P, et al. 2016. Large flux of iron from the Amery Ice Shelf marine ice to Prydz Bay, East Antarctica. J Geophys Res Oceans, 121(8): 6009-6020, doi:10.1002/2016JC011687.

Ho K C, Kang S H, Lam I H Y, et al. 2003. Distribution of *Alexandrium tamarense* in Drake Passage and the threat of harmful algal blooms in the Antarctic Ocean. Ocean Polar Res, 25(4): 625-631, doi:10.4217/opr.2003.25.4.625.

Huang W H, Yang X F, Zhao J, et al. 2022. Dissolved nutrient distributions in the Antarctic Cosmonaut Sea in austral summer 2021. Adv Polar Sci, 33(3): 267-290, doi:10.13679/j.advps.2022.0099.

Hunt B P V, Pakhomov E A, Trotsenko B G. 2007. The macrozooplankton of the Cosmonaut Sea, east Antarctica (30°E–60°E), 1987–1990. Deep Sea Res Part I Oceanogr Res Pap, 54(7): 1042-1069, doi:10.1016/j.dsr.2007.04.002.

IBM Corp. 2017. IBM SPSS statistics 25 core system user's guide. Armonk: IBM Corp. https://www.ibm.com/docs/SSLVMB_25.0.0.

Irigoien X, Huisman J, Harris R P. 2004. Global biodiversity patterns of marine phytoplankton and zooplankton. Nature, 429(6994): 863-867, doi:10.1038/nature02593.

Irion S, Christaki U, Berthelot H, et al. 2021. Small phytoplankton contribute greatly to CO_2-fixation after the diatom bloom in the Southern Ocean. ISME J, 15(9): 2509-2522, doi:10.1038/s41396-021-00915-z.

Jabre L J, Allen A E, McCain J S P, et al. 2021. Molecular underpinnings and biogeochemical consequences of enhanced diatom growth in a warming Southern Ocean. Proc Natl Acad Sci USA, 118(30): e2107238118, doi:10.1073/pnas.2107238118.

Jiang Z B, Liu J J, Zhu X Y, et al. 2020. Quantitative comparison of phytoplankton community sampled using net and water collection methods in the southern Yellow Sea. Reg Stud Mar Sci, 35: 101250, doi:10.1016/j.rsma.2020.101250.

Kolody B C, Smith S R, Zeigler Allen L, et al. 2022. Nitrogen and iron availability drive metabolic remodeling and natural selection of diverse phytoplankton during experimental upwelling. mSystems, 7(5): e00729-22, doi:10.1128/msystems.00729-22.

Krishnamurthy A, Moore J K, Mahowald N, et al. 2010. Impacts of atmospheric nutrient inputs on marine biogeochemistry. J Geophys Res Biogeosci, 115(G1): 2009JG001115, doi:10.1029/2009JG001115.

Krock B, Schloss I R, Trefault N, et al. 2020. Detection of the phycotoxin pectenotoxin-2 in waters around King George Island, Antarctica. Polar Biol, 43(3): 263-277, doi:10.1007/s00300-020-02628-z.

Lee S H, Kim B K, Yun M S, et al. 2012. Spatial distribution of phytoplankton productivity in the Amundsen Sea, Antarctica. Polar Biol, 35(11): 1721-1733, doi:10.1007/s00300-012-1220-5.

Lee Y, Park J, Jung J, et al. 2022. Unprecedented differences in phytoplankton community structures in the Amundsen Sea Polynyas, West Antarctica. Environ Res Lett, 17(11): 114022, doi:10.1088/1748-9326/ac9a5f.

Li Q M, Xiao W S, Wang R J, et al. 2021. Diatom based reconstruction of climate evolution through the Last Glacial Maximum to Holocene in the Cosmonaut Sea, East Antarctica. Deep Sea Res Part II Top Stud Oceanogr, 194: 104960, doi:10.1016/j.dsr2.2021.104960.

Li Y H, Zhao J, Li D, et al. 2024. Factors controlling the phytoplankton crops, taxonomic composition, and particulate organic carbon stocks in the Cosmonaut Sea, East Antarctica. J Oceanol Limnol, 42(6): 1895-1908, doi:10.1007/s00343-024-3198-6.

Li Z Z, Luk H C, Arromrak B S, et al. 2024. Nitrogen source and availability regulate plastic population dynamics in the marine diatom *Thalassiosira weissflogii*. Mar Environ Res, 202: 106733, doi:10.1016/j.marenvres.2024.106733.

MacArthur R. 1955. Fluctuations of animal populations and a measure of community stability. Ecology, 36(3): 533-536, doi:10.2307/1929601.

Martin-Jézéquel V, Hildebrand M, Brzezinski M A. 2000. Silicon metabolism in diatoms: implications for growth. J Phycol, 36(5): 821-840, doi:10.1046/j.1529-8817.2000.00019.x.

McNaughton S J. 1967. Relationships among functional properties of Californian grassland. Nature, 216(5111): 168-169, doi:10.1038/216168b0.

Menden-Deuer S, Lessard E J. 2000. Carbon to volume relationships for dinoflagellates, diatoms, and other protist plankton. Limnol Oceanogr, 45(3): 569-579, doi:10.4319/lo.2000.45.3.0569.

Mendes C R B, de Souza M S, Garcia V M T, et al. 2012. Dynamics of phytoplankton communities during late summer around the tip of the Antarctic Peninsula. Deep Sea Res Part I Oceanogr Res Pap, 65: 1-14, doi:10.1016/j.dsr.2012.03.002.

Moreau S, Hattermann T, de Steur L, et al. 2023. Wind-driven upwelling of iron sustains dense blooms and food webs in the eastern Weddell Gyre. Nat Commun, 14(1): 1303, doi:10.1038/s41467-023-36992-1.

Mou W X, Yang G, Hao Q, et al. 2021. The zooplankton community in cosmonaut sea: community structure and environmental factors. Oceanol Limnol Sin, 52(4): 925-935, doi:10.11693/hyhz20210200043 (in Chinese with English abstract).

Nardelli S C, Gray P C, Stammerjohn S E, et al. 2023. Characterizing coastal phytoplankton seasonal succession patterns on the West Antarctic Peninsula. Limnol Oceanogr, 68(4): 845-861, doi:10.1002/lno.12314.

Olesen A J, Leithoff A, Altenburger A, et al. 2021. First evidence of the toxin domoic acid in Antarctic diatom species. Toxins, 13(2): 93, doi:10.3390/toxins13020093.

Orsi A H, Whitworth T, Nowlin W D. 1995. On the meridional extent and fronts of the Antarctic Circumpolar Current. Deep Sea Res Part I Oceanogr Res Pap, 42(5): 641-673, doi:10.1016/0967-0637(95)00021-W.

Pakhomov E A, Perissinotto R. 1996. Antarctic neritic krill *Euphausia crystallorophias*: spatio-temporal distribution, growth and grazing rates. Deep Sea Res Part I Oceanogr Res Pap, 43(1): 59-87, doi:10.1016/0967-0637(95)00094-1.

Pan B J, Vernet M, Manck L, et al. 2020. Environmental drivers of phytoplankton taxonomic composition in an Antarctic fjord. Prog Oceanogr, 183: 102295, doi:10.1016/j.pocean.2020.102295.

Pielou E C. 1966. The measurement of diversity in different types of biological collections. J Theor Biol, 13: 131-144, doi:10.1016/0022-5193(66)90013-0.

Qi Q Q, Hao Q, Yang G, et al. 2025. Diverse impacts of sea ice and ice shelf melting on phytoplankton communities in the Cosmonaut Sea, East Antarctica. Environ Res Lett, 20(1): 014003, doi:10.1088/1748-9326/ad975e.

R Core Team. 2024. R: A language and environment for statistical computing. Vienna: R Foundation for Statistical Computing. https://www.R-project.org.

Redfield A C. 1958. The biological control of chemical factors in the environment. Am Sci, 46(3): 230A, 205-230A, 221.

Rodrigues L C, Simões N R, Bovo-Scomparin V M, et al. 2015. Phytoplankton alpha diversity as an indicator of environmental changes in a neotropical floodplain. Ecol Indic, 48: 334-341, doi:10.1016/j.ecolind.2014.08.009.

Schlitzer R. 2012. Ocean Data View. Bremerhaven: Alfred Wegener Institute. http://odv.awi.de..

Shramik P, Rahul M, Suhas S, et al. 2013. Phytoplankton abundance and community structure in the Antarctic polar frontal region during austral summer of 2009. Chin J Oceanol Limnol, 31(1): 21-30, doi:10.1007/s00343-013-1309-x.

Skjoldal H R, Wiebe P H, Postel L, et al. 2013. Intercomparison of zooplankton (net) sampling systems: Results from the ICES/GLOBEC sea-going workshop. Prog Oceanogr, 108: 1-42, doi:10.1016/j.pocean.2012.10.006.

ter Braak C J F, Smilauer P. 2002. CANOCO reference manual and CanoDraw for Windows user's guide: software for canonical community ordinatio. Ithaca: Microcomputer Power. https://www.microcomputerpower.com.

Tyrrell T. 1999. The relative influences of nitrogen and phosphorus on oceanic primary production. Nature, 400(6744): 525-531, doi:10.1038/22941.

Westwood K J, Brian Griffiths F, Meiners K M, et al. 2010. Primary productivity off the Antarctic coast from 30°–80°E; BROKE-West survey, 2006. Deep Sea Res Part II Top Stud Oceanogr, 57(9/10): 794-814, doi:10.1016/j.dsr2.2008.08.020.

Wolf C, Frickenhaus S, Kilias E S, et al. 2013. Regional variability in eukaryotic protist communities in the Amundsen Sea. Antartic Science, 25(6): 741-751, doi:10.1017/s0954102013000229.

Xu Z L, Chen Y Q. 1989. Aggregated intensity of dominant species of zooplankton in autumn in the East China Sea and Yellow Sea. Chin J

Ecol, 8(4): 13-15, 19 (in Chinese with English abstract).

Yang G, Atkinson A, Pakhomov E A, et al. 2022. Massive circumpolar biomass of Southern Ocean zooplankton: Implications for food web structure, carbon export, and marine spatial planning. Limnol Oceanogr, 67(11): 2516-2530, doi:10.1002/lno.12219.

Yang S K, Zhou M, Cheng X H. 2024. Seasonal and interannual variability between upper ocean processes and the slope current in the region around the cosmonauts sea off east Antarctica. J Geophys Res Oceans, 129(2): e2023JC019636, doi:10.1029/2023JC019636.

Zoccarato L, Pallavicini A, Cerino F, et al. 2016. Water mass dynamics shape Ross Sea protist communities in mesopelagic and bathypelagic layers. Prog Oceanogr, 149: 16-26, doi:10.1016/j.pocean.2016.10.003.